Phase-field modeling of fracture in liquid

Valery I. Levitas, Alexander V. Idesman, and Ameeth K. Palakala

Citation: Journal of Applied Physics **110**, 033531 (2011); doi: 10.1063/1.3619807
View online: http://dx.doi.org/10.1063/1.3619807
View Table of Contents: http://scitation.aip.org/content/aip/journal/jap/110/3?ver=pdfcov
Published by the AIP Publishing

Phase-field modeling of fracture in liquid

Valery I. Levitas,[1,a)] Alexander V. Idesman,[2] and Ameeth K. Palakala[2]
[1]*Departments of Mechanical Engineering, Aerospace Engineering, and Material Science and Engineering, Iowa State University, Ames, Iowa 50011, USA*
[2]*Department of Mechanical Engineering, Texas Tech University, Lubbock, Texas 79409, USA*

(Received 31 March 2011; accepted 27 June 2011; published online 11 August 2011)

Phase-field theory for the description of the overdriven fracture in liquid (cavitation) in tensile pressure wave is developed. Various results from solid mechanics are transferred into mechanics of fluids. Thermodynamic potential is formulated that describes the desired tensile pressure–volumetric strain curve and for which the infinitesimal damage produces infinitesimal change in the equilibrium bulk modulus. It is shown that the gradient of the order parameter should not be included in the energy, in contrast to all known phase-field approaches for any material instability. Analytical analysis of the equations is performed. Problems relevant to the melt-dispersion mechanism of the reaction of nanoparticles on cavitation in spherical and ellipsoidal nanoparticles with different aspect ratios, after compressive pressure at its surface sharply dropped, are solved using finite element method. Some nontrivial features (lack of fracture at dynamic pressure much larger than the liquid strength and lack of localized damage for some cases) are obtained analytically and numerically. Equations are formulated for fracture in viscous liquid. A similar approach can be applied to fracture in amorphous and crystalline solids. © *2011 American Institute of Physics*. [doi:10.1063/1.3619807]

I. INTRODUCTION

Liquid can withstand a high tensile pressure for a short time after which it fractures with appearance of bubbles filled with gas at phase equilibrium pressure. In contrast to boiling, bubbles appear not due to liquid–gas transformation but due to bonds breaking between atoms, i.e., their separation at the distance when molecules stop interacting. Cavitation was studied in classical works by Zeldovitch[1] and Fisher[2] as a nucleation problem and the rate of bubble appearance versus tensile pressure and temperature was determined. More recent studies are presented, for example., in Refs. 3–9. In various applications at the nanoscale (e.g., for cavitation in rarefaction waves during laser ablation[10] or in Al nanoparticles after dynamic oxide shell fracture[11–13]), it is desirable to model nucleation and growth of individual bubbles without any assumptions about nucleation places, bubble shapes, and their evolution. Note that metallic nanoparticles (e.g., nickel and aluminum) can withstand tensile pressure of several GPa during tens of picoseconds.[8,10,12] Molecular dynamics simulation can solve this problem (see, e.g., Refs. 8 and 10), but it has well-known limitations on size of the system and process duration. Phase-field theory has much weaker limitations on the system size and process time but it requires development of the proper thermodynamic potential and kinetics. There are two main items in any phase-field approach. (1) An order parameter η is introduced that describes two (meta) stable states of material and material instability that leads to transformation from one state to another. (2) The evolution of the system is described by the phase-field equation for η that leads to formation of finite-width (diffuse) interfaces between regions with different (meta) stable states, in contrast to discontinuity surfaces in a sharp-interface approach. While for evolution of cracks in solids phase-field theory was recently intensively developed and applied to various problems,[14–18] and in more advanced form (but for quasistatic deformation) in Refs. 19 and 20, we are not aware of any similar work for fracture of liquid. The goal of this paper is to develop phase-field theory and finite element method (FEM) simulation for overdriven fracture of liquid in tensile pressure wave. By overdriven we mean that applied tensile pressure exceeds the ultimate strength of liquid, and thermal fluctuations are not necessary for nucleation. At the same time, if a traditional stochastic term that mimics fluctuations is introduced in our phase-field equation, this equation will be applicable for the description of thermally activated fracture well below the ultimate strength of the liquid. While we are inspired by the above-mentioned papers for solids, our approach for liquid has several basic distinguishing points:

(a) Thermodynamic potential is developed that describes the desired tensile pressure $p > 0$–volumetric strain ε_0 curve (Fig. 1) and for which the infinitesimal damage produces infinitesimal change in the equilibrium bulk modulus (in contrast to Refs. 19 and 20). Note that the tensile pressure p is considered as a positive one, which is opposite to the usual convention but convenient for study of cavitation.
(b) The gradient of the order parameter does not contribute to the energy, in contrast to all known phase-field approaches for any material instability, like phase transformations, twinning, and dislocation evolution. Lack of the term with gradient of the order parameter does not prevent our theory from being a phase-field theory because it still possesses the two main features of any phase-field theory mentioned earlier.
(c) Bubble nucleation was treated here while pre-existing cracks or fixed void were studied in Refs. 14, 15, and 17–20.

[a)]Electronic mail: vlevitas@iastate.edu.

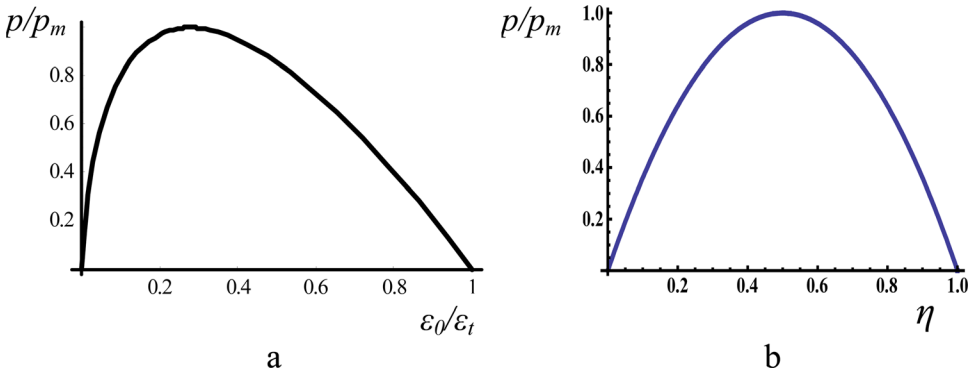

FIG. 1. (Color online) (a) Equilibrium tensile pressure–volumetric strain curve [Eqs. (5) and (10)] and (b) pressure–order parameter curve [Eq. (10)].

The obtained results have implications on the development of phase-field theory of fracture (void and crack nucleation and growth) in crystalline and amorphous solids and on general phase-field theory as well. In addition, the dynamic equations of motion are used instead of static equations, which are used in most similar papers.[19,20] Static equations allow one to consider fracture of solids but they are completely unrealistic for fracture of liquid. FEM was used for problem solution (in contrast to Refs. 14–20), which allows one to easily include arbitrary boundary conditions, large displacement and strains, dynamic formulation, and more sophisticated constitutive equations (when required). Problems on cavitation in spherical and ellipsoidal particles with different aspect ratios after compressive pressure at its surface sharply dropped are solved. They are important for the development and understanding of the melt-dispersion mechanism of reaction of aluminum nanoparticles.[11–13] Our analytical study revealed that liquid can withstand, without fracture, dynamic pressure that significantly exceeds the liquid strength and that damage does not localize in some cases; numerical results confirm these findings.

The paper is organized as follows. Phase-field model for fracture in ideal liquid is developed in Sec. II. The total system of equations is presented in Sec. III. Section IV contains analytical estimates for fracture in liquid. FEM solutions for cavitation within spherical and ellipsoidal particles are obtained and analyzed in Sec. V. Comparison with alternative phase-field approaches to fracture in solids is presented in Sec. VI. Generalization for fracture in viscous liquid is given in Sec. VII. Section VIII contains concluding remarks.

II. PHASE-FIELD MODEL FOR FRACTURE IN LIQUID

Thermodynamic derivations. The equilibrium tensile pressure p–volumetric strain ε_0 curve for an elemental volume of liquid has stable increasing and unstable decreasing branches and $p=0$ for $\varepsilon_0 \geq \varepsilon_t$ (Fig. 1), where ε_t is the stress-free volumetric strain corresponding to completely broken liquid and zero pressure. Let us introduce the order parameter η (internal variable) characterizing the bond breaking process, namely, $\eta=0$ corresponds to "undamaged" liquid and $\eta \geq 1$ corresponds to completely broken bonds and zero thermodynamically equilibrium pressure. The nonequilibrium, nonlinear equation of state,

$$p(\varepsilon_0,\eta)=K[\varepsilon_0-\varepsilon_t\varphi(\eta)], \tag{1}$$

describes relaxation of pressure for undamaged liquid $p=K\varepsilon_0$ due to evolution of the order parameter η (bond breaking), where K is the bulk modulus and $\varphi(\eta)$ is a monotonic function to be determined. Since for undamaged liquid $(\eta=0)$ $p=K\varepsilon_0$, then $\varphi(0)=0$. Without loss of generality we put $\varphi(1)=1$. Since nothing changes after complete fracture $(\eta \geq 1)$, then one has to accept that $\varphi=1$ for $\eta \geq 1$. Note that for solids, the term $\varepsilon_t\varphi(\eta)$ is called eigen (transformation) strain and it is used in Refs. 19 and 20 to describe cracks; the difference $\varepsilon_0-\varepsilon_t\varphi(\eta)$ is the elastic volumetric strain.

To obtain an equilibrium tensile pressure p–volumetric strain ε_0 curve shown in Fig. 1, we will start with the simplest expression for the internal energy,

$$U=0.5K[\varepsilon_0-\varepsilon_t\varphi(\eta)]^2+Qf(\eta), \tag{2}$$

where the first term represents the elastic energy and $Qf(\eta)$ is the cohesion energy. Here Q is the maximum cohesion energy and $f(\eta)$ is a function to be determined. For function $f, f(0)=0$ (i.e., for $\eta=0$ there is no energy associated with the damage) and $f(\eta)=1$ for $\eta \geq 1$, i.e., the cohesion energy reaches maximum value Q at $\eta=1$ corresponding to complete fracture and then it is independent of η for $\eta \geq 1$ (since fluid is already completely damaged). To provide a smooth conjugation of two branches of U function at $\eta=1$, we put $df(1)/d\eta=0$.

To be able to use pressure p as an independent variable, it is convenient to introduce the Gibbs energy,

$$\Phi=U-p\varepsilon_0=-0.5p^2/K-p\varepsilon_t\varphi(\eta)+Qf(\eta), \tag{3}$$

where Eq. (1) was used. Conditions of thermodynamic equilibrium,

$$\varepsilon_0=-\frac{\partial\Phi}{\partial p}, \quad \frac{\partial\Phi}{\partial\eta}=0, \tag{4}$$

result in, for $0 \leq \eta \leq 1$,

$$\varepsilon_0=\frac{p}{K}+\varepsilon_t\varphi(\eta), \tag{5}$$

$$p=\frac{Q}{\varepsilon_t}\frac{df}{d\eta}\Big/\frac{d\varphi}{d\eta}. \tag{6}$$

Equations (5) and (6) are the parametric representation (with the parameter η) of the equilibrium pressure p–volumetric strain ε_0 curve (Fig. 1). Equation (5) is equivalent to Eq. (1), which justifies our choice of the potential U in Eq. (2). Equation (6) results in $p=0$ for $\eta \geq 1$.

Let us derive the simplest expressions for the functions $f(\eta)$ and $\varphi(\eta)$ in order to describe a typical equilibrium $p-\varepsilon_0$ curve in Fig. 1. Since in the initial state with $p=\varepsilon_0=0$ damage should be absent, Eq. (6) should satisfy the condition $p_{|\eta=0}=0$. It means that (a) $df/d\eta_{|\eta=0}=0$ and (b) f has to be higher degree polynomial than φ at $\eta \to 0$. The next important constraint,

$$\frac{dp}{d\varepsilon_{0|\eta=0}}=K, \tag{7}$$

means that introduction of the order parameter does not affect the initial bulk modulus in the undamaged state, i.e., that infinitesimal damage causes infinitesimal change in the bulk modulus. Equation (7) coincides with differentiated equation (5),

$$\frac{d\varepsilon_0}{d\eta}=\frac{1}{K}\frac{dp}{d\eta}+\varepsilon_t\frac{d\varphi}{d\eta}, \tag{8}$$

at $\eta=0$ when $d\varphi/d\eta_{|\eta=0}=0$. We choose the simplest expression $\varphi=\eta^2$, which satisfies all conditions that we need [$\varphi(0)=0$, $\varphi(1)=1$, and $d\varphi/d\eta_{|\eta=0}=0$].

Then f has to start with η^3 to give $p_{|\eta=0}=0$ in Eq. (6). The minimal degree polynomial $f=\eta^3(4-3\eta)$ satisfies this requirement and $f(1)=1$ and $df(1)/d\eta=0$.

Final expressions. Thus, the desired thermodynamic potential is

$$\begin{aligned}\Phi&=-\frac{1}{2}\frac{p^2}{K}-p\varepsilon_t\eta^2+Q\eta^3(4-3\eta) \quad \text{for} \quad 0\leq\eta<1\\ \Phi&=-\frac{1}{2}\frac{p^2}{K}-p\varepsilon_t\eta^2+Q \quad \text{for} \quad \eta\geq 1.\end{aligned} \tag{9}$$

Equation (6) simplifies to

$$p=4p_m(1-\eta)\eta \tag{10}$$

with the maximum tensile pressure $p_m=1.5Q/\varepsilon_t$ [Fig. 1(b)]. Initiation of fracture in the absence of fluctuations is associated with material instability (when order parameter can spontaneously grow under constant or even reducing stress), see the decreasing branch of $p(\eta)$ plot in Fig. 1(b). Thermodynamic instability condition, $d^2\Phi/d\eta^2=0$, leads to $\eta_c=1/3+\sqrt{2Q(2Q-p\varepsilon_t)}/(6Q)$, which in combination with Eq. (10) for p results in the following values of the critical η_c and the corresponding ideal liquid strength:

$$\eta_c=0.5, \quad p=p_m=1.5Q/\varepsilon_t. \tag{11}$$

Strain corresponding to instability is determined by substituting η_c and p_m into Eq. (5),

$$\varepsilon_c=0.25[\varepsilon_t+6Q/(K\varepsilon_t)]=0.25\varepsilon_t+p_m/K. \tag{12}$$

Exclusion of η from Eqs. (5) and (10) leads to the desirable equilibrium $p-\varepsilon_0$ curve shown in Fig. 1(a). The above equations (9)-(12) give the generic thermodynamic potential and pressure–volumetric strain curve. When experimental or atomistic data on the pressure–volumetric strain curve are available for tensile pressure (see, e.g., Refs. 8 and 9), then these expressions can be made more precise, while satisfying the same mandatory conditions.

Kinetic equation. For nonequilibrium processes, the evolution equation for the order parameter in Eulerian description is taken in the form of linear relationship between generalized thermodynamic force and conjugate rate,

$$\frac{D\eta}{Dt}=-\chi\frac{\partial\Phi}{\partial\eta}=\frac{3\eta}{\tau_f}[p/p_m-4\eta(1-\eta)H(1-\eta)], \tag{13}$$

where H is the Heaviside step function, $\chi>0$ is the kinetic coefficient, and $\tau_f=1/(\chi Q)$ is characteristic fracture time. We put $\chi=0$ for $\eta<0$ to avoid negative η.

III. TOTAL SYSTEM OF EQUATIONS

Equations (5) and (13) are supplemented by the equation of motion for ideal liquid,

$$\nabla p=\rho\frac{D\mathbf{v}}{Dt}, \tag{14}$$

continuity equation,

$$\frac{D\rho}{Dt}+\rho\nabla\cdot\mathbf{v}=0, \tag{15}$$

and kinematic equation,

$$\varepsilon_0=\rho_0/\rho-1, \tag{16}$$

where the Eulerian description is used, $\mathbf{v}$ is the velocity vector, ∇ is the gradient operator, and ρ and ρ_0 are the current mass density and the mass density of the undamaged liquid in the undeformed state.

Dimensionless form. Let us introduce the sound speed in the undamaged liquid in the undeformed state $c=\sqrt{K/\rho_0}$, the acoustic time $t_a=R/c$, dimensionless time $\bar{t}=t/\tau_f$, and acoustic time $\bar{t}_a=t_a/\tau_f$, dimensionless velocity $\bar{\mathbf{v}}=\mathbf{v}/c$, pressure $\bar{p}=p/p_m$, position vector $\bar{\mathbf{r}}=\mathbf{r}/R$, gradient operator $\bar{\nabla}=R\nabla$, density $\bar{\rho}=\rho/\rho_0$, and bulk modulus $\bar{K}=K/p_m$, where R is the characteristic size (in particular, the radius of the spherical particle below). Then the total system of equations includes

$$\bar{p}=\bar{K}(\varepsilon_0-\varepsilon_t\eta^2), \tag{17}$$

$$\varepsilon_0=1/\bar{\rho}-1, \tag{18}$$

$$\frac{D\bar{\rho}}{D\bar{t}}+\frac{\bar{\rho}}{\bar{t}_a}\bar{\nabla}\cdot\mathbf{v}=0, \tag{19}$$

$$\bar{\nabla}(\varepsilon_0-\varepsilon_t\eta^2)=\bar{\rho}\bar{t}_a\frac{D\bar{\mathbf{v}}}{D\bar{t}}, \tag{20}$$

$$\frac{D\eta}{D\bar{t}}=3\eta[\bar{p}-4\eta(1-\eta)H(1-\eta)]. \tag{21}$$

In general, the stochastic term should be added to the left-hand side of Eq. (21) to mimic thermal fluctuations and

cause appearance of the critical nucleus. In the paper, we focus on the overdriven fracture, i.e., when $p > p_m$ and any perturbation will result in nucleation. It can be introduced through initial condition $\eta_0 > 0$, because for $\eta_0 = 0$ one obtains $\dot{\eta} = 0$ in Eq. (21).

Geometrically linear case. For the case when displacement and volumetric strain are relatively small (for example, for $\varepsilon_t \leq 0.1$ and initial stage of flow with the bubbles), the difference between Lagrangian and Eulerian approaches is negligible, differentiation with respect to time and space variable is commutative, and one can reformulate the problem in terms of particles displacements $\boldsymbol{u}$. Thus, introducing dimensionless displacements $\bar{\mathbf{u}} = \mathbf{u}/R$, instead of three equations, Eqs. (18)–(20), one obtains two equations,

$$\varepsilon_0 = \bar{\nabla} \cdot \bar{\mathbf{u}}, \tag{22}$$

$$\bar{\nabla}(\varepsilon_0 - \varepsilon_t \eta^2) = \bar{t}_a^2 \frac{d^2 \bar{\mathbf{u}}}{d\bar{t}^2}, \tag{23}$$

and $\bar{\rho} \simeq 1$. Equations (17), (21)–(23) look like phase-field theory of fracture of elastic solids with zero shear moduli and small displacements and volumetric strains. However, our phase-field equation (21) differs from that used for solids in Refs. 14–20.

IV. ANALYTICAL ESTIMATES

A. Fracture at constant pressure

First, let us focus on the solution to Eq. (21) in a local material point for constant pressure $\bar{p}$ and its interpretation with the help of Fig. 1. After nucleation, for any constant $\bar{p} \leq 1$, solution of Eq. (21) for η tends to the stationary solution $\bar{p} = 4\eta(1-\eta)$ [which coincides with Eq. (10)] shown in Fig. 1(b). For $\eta \leq 0.5$, liquid exhibits stable equilibrium behavior with $\bar{p} \leq 1$, for $\eta > 0.5$ the stationary solution is unstable, i.e., η grows with decrease in $\bar{p}$.

For $\bar{p} > 1$, there is no stationary solution for η and unstable fracture starts. Growth in η in turn leads to pressure relaxation [see Eq. (17)] to unstable branch of stationary solution for η, $\bar{p} = 4\eta(1-\eta)$, or to $\eta \geq 1$ and $\bar{p} = 0$. For $\eta \geq 1$, Eq. (21) simplifies to

$$\frac{d\eta}{d\bar{t}} = 3\eta\bar{p}, \tag{24}$$

i.e., η will evolve until the stationary value corresponding to $\bar{p} = 0$. If further evolution of η occurs at $\bar{p} = 0$, then evolution of η is not determined by Eq. (21) (since fracture is completed) but by condition $\bar{p} = 0$ in Eq. (17), i.e., by

$$\eta = \sqrt{\frac{\varepsilon_0}{\varepsilon_t}}. \tag{25}$$

This process does not represent fracture but hydrodynamic expansion of cavity.

Healing. Note that if pressure instantaneously drops to zero, elastic unloading occurs with bulk modulus K, like for elastoplastic material. Then for $0 < \eta < 1$ material will heal [$\dot{\eta} < 0$ in Eq. (21)] and for $\eta \geq 1$ will not [see Eq. (24)]. Healing of completely fractured liquid can start when $\bar{\varepsilon}_0 < 1$, which leads to $\eta < 1$ [Eq. (25)] and $\dot{\eta} < 0$ according to Eq. (21). Integral of Eq. (21) at $p = 0$ leads to the following equation for healing:

$$\bar{t} = 4[F(\eta) - F(\eta_0)] \quad \text{with} \quad F = \frac{1}{\eta} + \ln\frac{1-\eta}{\eta}, \quad \bar{\varepsilon}_0 = \eta^2. \tag{26}$$

Healing at constant $\bar{\varepsilon}_0$ is described by Eq. (28), see the following.

B. Very fast fracture, $\bar{t}_a \gg 1$

We will focus on the case $\bar{t}_a \gg 1$ (i.e., when fracture time is much shorter than the acoustic time) and when the equation of motion, Eq. (20), can be simplified to $d\bar{\mathbf{v}}/d\bar{t} \simeq 0$ and Eq. (19) simplifies to $\bar{\rho} \simeq const$. Thus, fracture can be considered as a quasistatic process at $\varepsilon_0 = const$. Then substitution of Eq. (17) into Eq. (21) results in

$$\frac{d\eta}{d\bar{t}} = 3\eta\left[K_t(\bar{\varepsilon}_0 - \eta^2) - 4\eta(1-\eta)H(1-\eta)\right], \tag{27}$$

with $K_t = \bar{K}\varepsilon_t$ and $\bar{\varepsilon}_0 = \varepsilon_0/\varepsilon_t$, i.e., $\bar{p} = K_t(\bar{\varepsilon}_0 - \eta^2)$.

(a) For $\eta \leq 1$, $H(1-\eta) = 1$ and Eq. (27) allows the closed form solution

$$\bar{t} = \frac{(K_t - 4)^3}{2K_t\bar{\varepsilon}_0 B}[N(\eta) - N(\eta_0)], \qquad N = \ln[\eta^{a-b}|\eta - a|^b|b - \eta|^{-a}] \tag{28}$$

with

$$B = \sqrt{4 - 4K_t\bar{\varepsilon}_0 + K_t^2\bar{\varepsilon}_0}, \quad a = \frac{-2-B}{K_t - 4}, \quad b = \frac{-2+B}{K_t - 4}, \tag{29}$$

where a and b are the roots of square equation

$$\bar{p} = K_t(\bar{\varepsilon}_0 - \eta^2) = 4\eta(1-\eta), \tag{30}$$

corresponding to stationary η. The condition that B is a real number is automatically satisfied for $K_t > 4$ and leads to $\bar{\varepsilon}_0 \leq 4/[K_t(4-K_t)]$ for $K_t < 4$. Since $4/[K_t(4-K_t)] \geq 1$, then the limitation for the case with $K_t < 4$, $\bar{\varepsilon}_0 \leq 1$ is not restrictive, because we consider the case $\eta \leq 1$. For $K_t > 4$, $a < 0$, and the root $\eta = b$, $0 \leq b \leq 1$, represents the only realistic stationary solution, which is shown in Fig. 2 versus $\bar{\varepsilon}_0$ for various $K_t > 4$. For $K_t \to 4$, the relationship $b(\bar{\varepsilon}_0) = \bar{\varepsilon}_0$ is linear; for any $K_t > 4$, one has $b(0) = 0$ and $b(1) = 1$. The stationary solution b weakly depends on K_t and, for example, for $K_t = 100$ and $K_t = 1000$, the difference in $b(\bar{\varepsilon}_0)$ is invisible. For $K_t < 4$, one has $b(0) = 0$ and $b(1) = (|K_t - 2| - 2)/(K_t - 4)$; the last equation simplifies to $b(1) = 1$ for $2 \leq K_t < 4$ and to $b(1) = K_t/(4 - K_t)$ for $K_t < 2$.

The first root $a(\bar{\varepsilon}_0)$ does not give realistic stationary solutions $0 \leq a \leq 1$ for $K_t < 4$ as well. Indeed, $a(\bar{\varepsilon}_0)$ decreases with the growth of $\bar{\varepsilon}_0$; $a(0) = 4/(4 - K_t) > 1$;

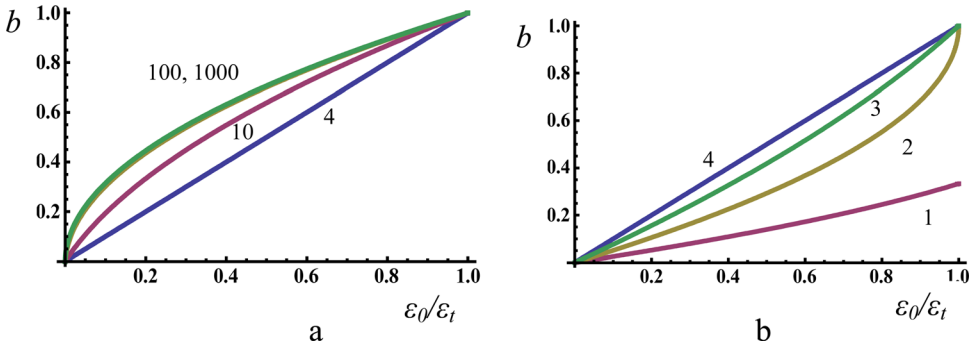

FIG. 2. (Color online) Stationary solutions $\eta = b$ [Eq. (29)] of the evolution equation (28) vs prescribed volumetric strain $\varepsilon_0/\varepsilon_t$ for various values of dimensionless bulk modulus K_t, shown near the curves: (a) for $K_t \geq 4$ and (b) for $K_t \leq 4$.

$a(1) = (|K_t - 2| + 2)/(4 - K_t)$; the last equation simplifies to $a(1) = 1$ for $K_t < 2$ and to $a(1) = K_t/(4 - K_t) > 1$ for $2 \leq K_t < 4$, i.e., $a > 1$ for all $K_t < 4$ and $\bar{\varepsilon}_0 \leq 1$, except $a(1) = 1$ for $K_t < 2$. However, for $K_t < 2$ one has $b(1) = K_t/(4 - K_t) < 1$, and nonstationary solution (28) tends to the smaller stationary solution $\eta = b$ for any initial conditions. Indeed, for $\bar{\varepsilon}_0 = 1$, if $\eta_0 < b$, then in Eq. (28) $d\eta/d\bar{t} > 0$ and solution tends to b; if $b < \eta_0 < 1$, then in Eq. (28) $d\eta/d\bar{t} < 0$ and solution tends to b again.

Summarizing, for any $\bar{\varepsilon}_0 \leq 1$, K_t, and initial value η_0, the nonstationary solution (28) exponentially tends to the stationary solution $\eta = b$ [Eq. (29)] with corresponding stationary pressure $\bar{p} = 4b(1 - b)$.

For $K_t = 4$ and $\eta \leq 1$, Eq. (27) takes a form $d\eta/d\bar{t} = 12\eta(\bar{\varepsilon}_0 - \eta)$ and has solution

$$\eta = \frac{\eta_0 \bar{\varepsilon}_0 \exp(12\bar{\varepsilon}_0 \bar{t})}{\bar{\varepsilon}_0 + \eta_0[\exp(12\bar{\varepsilon}_0 \bar{t}) - 1]} \tag{31}$$

with stationary solutions (Fig. 2)

$$\eta = \bar{\varepsilon}_0, \quad \bar{p} = 4\bar{\varepsilon}_0(1 - \bar{\varepsilon}_0). \tag{32}$$

The important conclusion from the stationary solutions Eqs. (30) and (32) is that for initial $\eta_0 \leq 1$ and $\bar{\varepsilon}_0 < 1$, *fracture is not complete (i.e., $\bar{p} > 0$) even if initial $\bar{p}$ significantly exceeds 1, i.e., when the ideal liquid strength is exceeded*. The condition $\bar{\varepsilon}_0 \geq 1$ (i.e., $\bar{p} \geq K_t$, or, equivalently, $p > K\varepsilon_t$) is *necessary for complete fracture*.

(b) For $\eta \geq 1$, Eq. (27) reduces to $d\eta/d\bar{t} = 3\eta[K_t(\bar{\varepsilon}_0 - \eta^2)]$ with initial condition $\eta(\bar{t}^*) = 1$ at time t^* and it has a solution

$$\eta = \frac{\sqrt{\bar{\varepsilon}_0}}{\sqrt{(\bar{\varepsilon}_0 - 1)\exp[-6K_t\bar{\varepsilon}_0(\bar{t} - \bar{t}^*)] + 1}}, \tag{33}$$

which gives $\eta \geq 1$ for $\bar{\varepsilon}_0 \geq 1$ only. Substitution of Eq. (33) into Eq. (17) gives us an evolution for $\bar{p}$,

$$\bar{p} = \frac{K_t\bar{\varepsilon}_0}{1 + \exp[6K_t\bar{\varepsilon}_0(\bar{t} - \bar{t}^*)]/(\bar{\varepsilon}_0 - 1)}. \tag{34}$$

Stationary solutions for these equations are $\eta_{st} = \sqrt{\bar{\varepsilon}_0}$ and $\bar{p}_{st} = 0$, and time during which these solutions are reached is $\simeq 1/(K_t\bar{\varepsilon}_0)$.

Mechanical instability. Since for $\eta > 0.5$ the local equilibrium $p - \varepsilon_0$ curve has a decreasing branch, mechanical instability may occur in solution of a boundary-value problem. Note that the behavior of a material point is unstable under prescribed pressure but stable under prescribed local strain ε_0. For a finite volume, instability of a stationary solution usually exhibits itself in the form of strain localization. However, if $\bar{t}_a \gg 1$ (fast fracture) and a dynamic process occurs at almost constant ε_0 at each point, strain localization should be suppressed for the time interval while changes in ε_0 are small. Also, the characteristic size of a localized region is $l = c\tau_f$. Thus, if the size of a damaged region with $\eta > 0.5$ is smaller than l, strain localization will be suppressed as well. The suppression of localization due to the above-mentioned reasons is confirmed in our numerical simulations to follow.

When fracture time is comparable to or much longer than the acoustic time, analysis cannot be performed for a single material point and should be based on the solution of the complete system, Eqs. (17)–(21).

To summarize, several important conclusions can be drawn from the above-presented analytical solutions. For prescribed volumetric strain (which is the case for very fast fracture), fracture is not completed even when tensile pressure significantly exceeds the ideal liquid strength. Condition $p > K\varepsilon_t$ is necessary for complete fracture; otherwise, healing may occur. This is in contrast to the current treatment of cavitation, in which a bubble is introduced when pressure reaches some critical value (which is usually well below the ideal liquid strength[4–7])—i.e., overloading (overdriving) is impossible. Since fast fracture occurs at almost constant volumetric strain for which local mechanical behavior is stable, global mechanical instability in the form of localized damage may not occur even for the parameters corresponding to the decreasing branch of pressure–volumetric strain curve.

V. CAVITATION WITHIN SPHERICAL AND ELLIPSOIDAL PARTICLES: NUMERICAL SIMULATION

We will simulate cavitation under conditions described in the melt-dispersion mechanism for initiation of fast chemical reactions of aluminum nanoparticles covered by a thin alumina shell.[12] During fast heating and melting of nanoparticles, the volume change due to melting of Al induces pressure of 1 GPa in the melt and causes fracture and spallation of the oxide shell. A subsequent unloading wave creates significant tensile pressures in the melt resulting in cavitation and dispersion of small liquid Al clusters, the reaction of which is not limited by diffusion through oxide shell (in

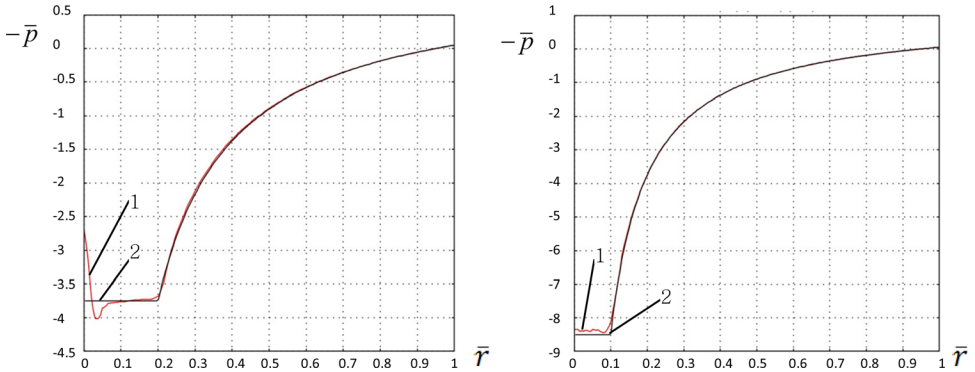

FIG. 3. (Color online) Comparison of numerical solution (1) and analytical solution (2) (Ref. 12) for the problem before cavitation.

contrast to traditional mechanisms). Here we consider the appearance of the first void in the melt. Solution to the system of equations (17)–(21) was found using FEM and code COMSOL.

We consider a liquid sphere of radius R that is initially in mechanical equilibrium under applied external compressive pressure $-p_0$ ($p_0 > 0$), i.e., initial velocity is zero. Initial value $\eta_0 = 0.03$ is distributed everywhere to start evolution of η. Let the magnitude of the compressive pressure at the boundary $\bar{r} = 1$ reduce linearly in time from p_0 to the final value p_f during the time t_s (e.g., during the time of oxide shell fracture[12]), after which it remains constant. During this process, the unloading wave propagates to the center and creates large tensile pressure, which causes cavitation. For spherical particle, cavitation starts at the center where the reflected wave causes the highest pressure. The effect of the heterogeneity of distribution and the magnitude of η_0 on the solution will be studied elsewhere. Some estimates of the effect of the magnitude of η_0 can be obtained from analytical solutions in Sec. IV.

Before fracture starts and evolution of the order parameter is negligible, we arrive at classical fluid dynamics equations. Then, solution depends on the different dimensionless time $\tilde{t} = t/t_a = \bar{t}/\bar{t}_a$ and pressure $\tilde{p} = p/p_0 = \bar{p}/\bar{p}_0$.

The following parameters have been used in calculations[12]: $\tilde{p}_f = 0.05$, $\tilde{t}_s = 0.2$, $\bar{p}_0 = 1$, $\bar{t}_a = 0.944$, $\varepsilon_t = 0.1$, and $\bar{K} = 71.1$. This leads to $K_t = 7.11$, the maximum tensile pressure in the central region of a sphere $\bar{p}_{\max} = 8.5$ (Fig. 4), the maximum value of strain $\varepsilon_{\max} = \bar{p}_{\max}/\bar{K} = 0.1195 > \varepsilon_t$, $\bar{\varepsilon}_{\max} = \varepsilon_{\max}/\varepsilon_t = 1.195 > 1$, stationary value $\eta_{\text{st}} = \sqrt{\bar{\varepsilon}_{\max}} = 1.093$, and time during which the solution changes from $\eta = 1$ to η_{st} is $\simeq 1/(K_t\bar{\varepsilon}_{\max}) = 0.118$.

FEM solution reproduces well an analytical solution to fluid dynamics problem found in Ref. 12 (Fig. 3). In particular, for $\tilde{t} = 1$ (when wave reached the particle center) and in the region $0 \le \bar{r} \le \tilde{t}_s$, the tensile pressure is constant and equal to its maximum value in the interval $\tilde{t} \le 1$,

$$\tilde{p}_{\diamondsuit} = -1 + (1 - \tilde{p}_f)/\tilde{t}_s. \tag{35}$$

For $\tilde{t} = 1 + 0.5\tilde{t}_s$ (i.e., in the reflected wave) and in the region $0 \le \bar{r} \le 0.5\tilde{t}_s$, pressure is constant and is equal to the maximum tensile pressure in the problem

$$\tilde{p}_{\max} = -1 + 2(1 - \tilde{p}_f)/\tilde{t}_s. \tag{36}$$

Also, for $\tilde{t} = 1$, velocity in the central part reaches its maximum value,[12]

$$\bar{v}_m = \frac{p_0}{2K}\frac{(1 - \tilde{p}_f)}{\tilde{t}_s}, \tag{37}$$

while for $\tilde{t} = 1 + 0.5\tilde{t}_s$ it is zero everywhere. Note that for $\tilde{t} = 1$, velocity has jump at $r = 0$ from zero (according to boundary condition) to the value determined by Eq. (37).[12]

Triangular finite elements with quadratic displacement and velocity approximation have been used. To study mesh

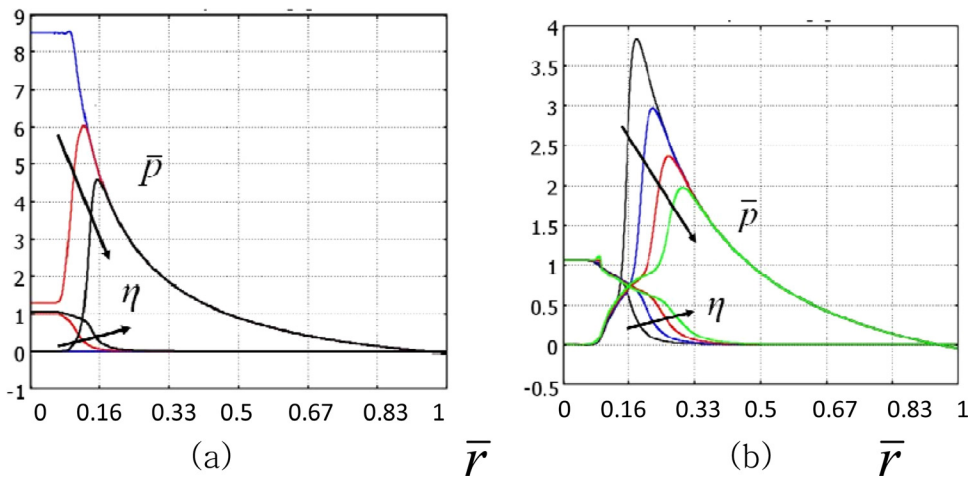

FIG. 4. (Color online) Evolution of the tensile pressure and the order parameter in a spherical particle: (a) initial stage; (b) after appearance of a void.

dependence of the solution, two meshes consisting of 7936 finite elements with 48 147 mechanical degrees of freedom and 31 744 elements with 191 523 mechanical degrees of freedom were used for a quarter of axisymmetric cross section. The solutions for the order parameter for the two meshes practically coincided, especially when η exceeded 1 at the center of the sphere.

Evolution of the pressure distribution and the order parameter is shown in Fig. 4. At time $\tilde{t} = 1 + 0.5\tilde{t}_s = 1.1$ (when tensile pressure $\bar{p} = 8.5$ is maximal and particles velocity is zero), there is still no visible change in the order parameter, despite very high tensile pressures. However, at $\tilde{t} = 1.136$, $\eta = 1$ at the center of particle and pressure in this region dropped homogeneously to 1.3. At $\tilde{t} = 1.154$, while η has grown very little to $\eta_{st} = 1.093$, pressure in this region reached its thermodynamically equilibrium value 0, which is equivalent to the appearance of a hole. Pressure drop generates an additional unloading wave. Diameter of the hole does not change during calculation time $\tilde{t} = 1.21$. Near the hole, pressure reduces and the order parameter grows until both of them reached thermodynamically equilibrium values $\bar{p} = 4\eta(1-\eta)$ determined by Eq. (10). While the local equilibrium is thermodynamically unstable under prescribed pressure, there is not any instability and strain localization. According to our discussions in Sec. IV.B, there are two reasons for the lack of strain localization:

(1) Actual time during which damage evolution has occurred is ten times smaller than the acoustic time, i.e., damage occurred under almost constant ε_0 at each point. Local solution is stable under prescribed ε_0.
(2) The size of the potential localization zone is $l = c\tau_f = R\tau_f/t_a = R/\bar{t}_a = 1.06R$ and is much larger than the actual damaged zone with $\eta > 0.5$ in Fig. 4.

The solution to the same problem but for ellipsoidal particles with aspect ratio $a = 1.2$ is presented in Fig. 5. Maximum tensile pressure reduces with growing aspect ratio ($\bar{p} = 7.55 > K_t$ for $a = 1.2$ and $\bar{p} = 2.98 < K_t$ for $a = 2$), which slows the growth of the order parameter. While for $a = 1.2$ a noncircular hole appeared at the center of particle (i.e., η reached 1 and pressure dropped to zero), for $a = 2$ the order parameter did not exceed 0.7 and pressure did not reach zero, i.e,. the hole did not appear. Concerning the melt-dispersion mechanism,[12] small deviation from spherical shape does not prevent cavitation but for large aspect ratios this mechanism cannot be initiated.

The typical order of magnitude of ideal strength of liquid metals is $p_m = 1$GPa, while complete fracture does not occur for $p < K\varepsilon_t = 7.11$GPa on the time scale of 1ps. Indeed, dynamic tensile pressure can significantly exceed the liquid strength without causing complete fracture. For Ni, fracture of melt starts at 6 GPa.[10] Note that in Refs. 8 and 9 pressure was below theoretical strength (spinodal) of liquid, causing thermal fluctuations to be required for the bubble nucleation, as well as greatly increasing the fracture time.

VI. COMPARISON WITH ALTERNATIVE PHASE-FIELD APPROACHES

A. Comparison with the alternative potential

The potential in Refs. 19 and 20 for a crack in solid (adapted for $p - \varepsilon_0$ variables) is

$$\Phi = -0.5p^2/K - p\eta/d + Q\,\sin^2(0.5\pi\eta/\eta_c) \qquad (38)$$

with $Q = 2\eta_c^2 K/(\pi^2 d^2)$, non-normalized η and η_c and d as parameters. Comparison with Eq. (9) shows that $\varepsilon_t\varphi(\eta) = \eta/d$, i.e., $\varphi(\eta) = \eta$, which contradicts our requirements $d\varphi/d\eta_{|\eta=0} = 0$, derived from condition equation (7). Indeed, thermodynamic equilibrium conditions $\partial\Phi/\partial\eta = 0$ and $\varepsilon_0 = -\partial\Phi/\partial p$ result in

$$p = 0.5\frac{Qd\pi}{\eta_c}\sin\left(\frac{\pi\eta}{\eta_c}\right) \qquad (39)$$

or for small η in

$$p \simeq 0.5\eta\frac{Qd\pi^2}{\eta_c^2} = K\frac{\eta}{d}, \quad \varepsilon_0 = \frac{p}{K} + \frac{\eta}{d}. \qquad (40)$$

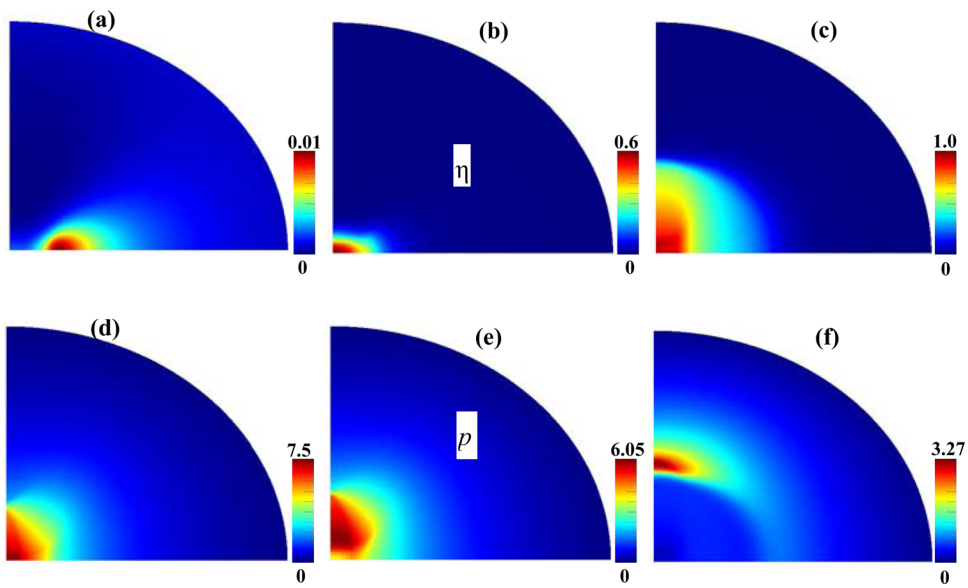

FIG. 5. (Color online) Evolution of the order parameter (a)–(c) and the tensile pressure (d)–(f) in an ellipsoidal particle with $a = 1.2$.

Excluding η from these two equations, we obtain $\varepsilon_0 = 2p/K$. At the same time for nonequilibrium (fast) loading when $\dot{\eta} = 0$, $\varepsilon_0 = p/K$, i.e., the equilibrium bulk modulus in Refs. 19 and 20 is two times smaller than the bulk modulus without initiation of fracture, which is contradictory.

Note that the nonlinear equilibrium $p(\varepsilon_0)$ curve for cracks in Refs. 14–18 was described in terms of variable elastic modulus rather than in terms of eigen strain.

B. Lack of the gradient energy

Usually, in all phase-field approaches (for example, for fracture, phase transformations, and twinning), an additional gradient energy term, $0.5\beta\nabla\eta \cdot \nabla\eta$ with $\beta > 0$ as the coefficient, is added to Φ, which results in Ginzburg–Landau equation [i.e., in the additional Laplacian term $\beta\Delta\eta$ in Eq. (13), see Refs. 14–18]. Gradient energy is concentrated near the newly formed free surface and reproduces interface energy. However, in our approach, the introduction of gradient energy will lead to a double count of cohesive energy and, consequently, to violation of the energy balance. Indeed, when crack appears in solid, stress work is equal to the cohesion energy which is stored in the interplanar volume.[19,20] Surface energy is defined in terms of cohesion energy but it is not added to the energy balance.[19,20] Similarly, here cohesion energy QV is stored in a hole of the volume V, so gradient (surface) energy cannot be added.

Also, while without gradient energy material instability starts at each material point independently when $p > p_m$, gradient energy promotes interface propagation for any pressure not equal to thermodynamic equilibrium (Maxwell) pressure. That is why the propagating crack in Refs. 14–18 increases its width due to phase transformation between solid phase and gas (or vacuum, or soft phase) inside the crack, which is not physical for actual cracks. In Refs. 19 and 20, gradient energy is formulated in a way that it appears at the crack tip only but not at crack faces. This contribution determines the line tension energy (rather than surface energy) and the crack core radius, similar to those for dislocations.[21] It is found in Refs. 19 and 20 that the gradient energy produces a weak effect on the solution of the problems under study. Note that in the cohesive zone models for crack,[22,23] gradient energy is absent.

We are not aware of phase-field modeling of any material instability (like phase transformations, twinning, and dislocation evolution) at the nanoscale that did not use gradient energy and the corresponding term in kinetic equation for order parameter. At the macroscale, we dropped gradient energy in phase-field modeling phase transformations,[24,25] because surface energy is not important for large volumes and interface width is negligible. For problems on damage and shear band localization in solids, strain gradient energy is added to avoid an ill-posed boundary-value problem.[26] Indeed, otherwise, due to the lack of characteristic size in the problem formulation, thickness of a shear band is zero and drastic mesh dependence of the solution is observed. Adding strain gradient contribution to the energy introduces a characteristic size in the problem formulation and leads to the strain gradient regularization.

Despite the lack of gradient energy and corresponding regularization in our problem formulation, this does not lead to an ill-posed problem and sharp (zero thickness) interface; the problem is well posed due to the rate-type regularization in Eq. (13) and momentum equation (14), which introduces a characteristic length $l_f = c\tau_f$. This regularization is similar to strain-rate regularization in viscoplasticity.[27]

Lack of the term with the gradient of the order parameter does not prevent our theory from being a phase-field (Ginzburg–Landau) theory, because it still possesses the two main features of any phase-field theory mentioned in Sec. I. In fact, the Landau theory of the second-order phase transformations did not contain the gradient of the order parameter,[28,29] which was later introduced by Ginzburg. Our theory, based on potential (2), can be formally considered as a mixture-type theory with a volume fraction of broken phase η^2 (because volumetric transformation strain is proportional to η^2) and interaction (surface) energy $Qf(\eta)$. Then, omitting the gradient-type energy would be natural. However, the phase-field theory of fracture in Refs. 14,18 also was formulated as a mixture-type theory with the order parameters as concentration of soft phase or point defects. Still, in these works the gradient-type energy has been used, and we would need to justify why we do not use it in our mixture theory. Also, change in concentration in mixture theory corresponds to transformations between phases, which corresponds more to sublimation or vacancy diffusion to the free surface than to fracture. Instead, we would like to describe bond breaking in each material point independent of other points, and this was one more reason to remove the gradient term; see our earlier discussion.

VII. CAVITATION IN VISCOUS LIQUID

For viscous liquid, the nonhydrostatic stresses should be taken into account in the description of cavitation. At the macroscale, the cavitation criterion suggested by Joseph[4–7] is based on maximum tensile stress. The simplest way to do this within a phase-field approach is to substitute pressure in the transformation work term with the maximum tensile stress σ_1,

$$\Phi = -0.5p^2/K - \sigma_1\varepsilon_t\eta^2 + Q\eta^3(4-3\eta). \tag{41}$$

Then, the principle strains are $\varepsilon_i = -\partial\Phi/\partial\sigma_i$, i.e.,

$$\varepsilon_1 = p/3K + \varepsilon_t\eta^2, \quad \varepsilon_2 = \varepsilon_3 = p/3K, \quad \varepsilon_0 = p/K + \varepsilon_t\eta^2. \tag{42}$$

The evolution equation for the order parameter is similar to Eq. (13),

$$\frac{d\eta}{dt} = -\chi\frac{\partial\Phi}{\partial\eta} = \frac{3\eta}{\tau_f}\left[\frac{\sigma_1}{p_m} - 4\eta(1-\eta)H(1-\eta)\right], \tag{43}$$

but with σ_1 instead of p. Equation for stress tensor in liquid is

$$\sigma_{ij} = K(\varepsilon_0 - \varepsilon_t\eta^2)\delta_{ij} + \left[\nu\alpha_1(\eta)\frac{\partial v_k}{\partial x_k}\delta_{ij} + \frac{1}{2}\mu\alpha_2(\eta)\left(\frac{\partial v_i}{\partial x_j} + \frac{\partial v_j}{\partial x_i}\right)\right], \tag{44}$$

where δ_{ij} is the Kronecker delta symbol, ν and μ are volumetric and shear viscosities, and $\alpha_i(\eta)$ are the functions with the following properties: $\alpha_i(0) = 1$ and $\alpha_i = 0$ for $\eta \geq 1$. Thus, cavitation is governed by the maximum principal stress, which is consistent with macroscopic cavitation criterion in Refs. 4 and 5. Note that in Refs. 4 and 5, σ_1 is the stress before fracture while in our approach it is variable stress in the fracture zone during the fracture process. Potential interpretation problem is that the direction of the largest principal stress may vary during the fracture process, i.e., it may stretch different bonds. It may change by 90° when the middle principle stress became the largest one. However, according to the above-mentioned properties of the functions $\alpha_i(\eta)$, the viscosities and nonhydrostaticity reduce during the fracture. Note that in similar way, one can generalize the above-presented phase-field approach for liquid with more complex constitutive equations.

VIII. CONCLUDING REMARKS

To summarize, phase-field theory for the description of the fracture in liquid is developed. Various results from solid mechanics are transferred into mechanics of fluids. Note that the same thermodynamic potential as for viscous liquid can be used to model fracture of disordered solids (glasses), if we add energy of deviatoric stresses. It also can be used for each cleavage plane in theory[19,20] for fracture of single crystals to avoid jump-like reduction in elastic moduli when damage starts. In particular, quadratic, rather than linear dependence of the eigen (transformation) strain is crucial for this purpose. Stochastic contribution (the noise due to thermal fluctuations, which satisfies the dissipation-fluctuation theorem) can be trivially added. Large-strain formulation[30,31] and surface tension[32,33] can be incorporated as well. This work also stresses the importance of analyzing pressure (stress)–strain curve in any stress-related phase-field theory. Earlier,[34,35] we demonstrated this for martensitic phase transformations. One more general contribution to the phase-field theories is the demonstration that for some cases, the gradient energy term has to be omitted, since it double counts cohesive energy and causes unrealistic diffusive expansion of the fractured region. The only example that we aware of neglected gradient term is in our microscale phase-field theory of martensitic phase transformation,[24,25] because at the microscale surface energy and corresponding width of the diffuse interface are negligible. Note that as result of solution of dynamic nucleation problem an unexpected metastable phase of material was obtained. This is a gas-like state of a matter under zero pressure in which distance between molecules is greater than atomic interaction distance. However, its free energy is equal to Q and is greater than free energy of gas and liquid. As the next step, this phase will transform into a stable mixture of liquid and gas. This phase transformation should be described with a different order parameter and gradient (liquid–gas interface) energy should be included. This problem will be treated elsewhere. The effect of impurities, interfaces, and other nucleation sites for fracture can be easily introduced by reducing p_m and ε_t at their surface.

ACKNOWLEDGMENTS

V.I.L. wishes to thank B. Ganapathysubramanian for helpful discussions on this paper. The support of the NSF (CBET-0755236 and CMMI-0969143), ONR (N00014-08-1-1262), Air Force (FA9300-11-M-2008), ISU, and TTU for this research is gratefully acknowledged.

[1]Ya. B. Zeldovitch, Acta Physicochim. URSS **18**, 1 (1943).
[2]J. C. Fisher, J. Appl. Phys. **19**, 1062 (1948).
[3]C. E. Brennen, *Cavitation and Bubble Dynamics* (Oxford University Press, New York, 1995).
[4]D. D. Joseph, Phys. Rev. Lett. **51**, 1649 (1995).
[5]D. D. Joseph, J. Fluid Mech. **366**, 367 (1998).
[6]J. C. Padrino, D. D. Joseph, T. Funda, J. Wang, and W. A. Sirignano, J. Fluid Mech. **578**, 381 (2007).
[7]S. Dabiri, W. A. Sirignano, and D. D. Joseph, Phys. Fluids **19**, 072112 (2007).
[8]T. T. Bazhirov, G. E. Norman, and V. V. Stegailov, J. Phys.: Condens. Matter **20**, 114113 (2008).
[9]K. Davitt, A. Arvengas, and F. Caupin, EPL **90**, 16002 (2010).
[10]D. S. Ivanov and L. V. Zhigilei, Phys. Rev. B **68**, 064114 (2003).
[11]V. I. Levitas, B. Dikici, and M. L. Pantoya, Combust. Flame **158**, 1413 (2011).
[12]V. I. Levitas, B. W. Asay, S. F. Son, and M. L. Pantoya, J. Appl. Phys. **101**, 083524 (2007).
[13]V. I. Levitas, Combust. Flame **156**, 543 (2009).
[14]I. S. Aranson, V. A. Kalatsky, and V. M. Vinokur, Phys. Rev. Lett. **85**, 118 (2000).
[15]A. Karma, D. A. Kessler, and H. Levine, Phys. Rev. Lett. **87**, 45501 (2001).
[16]A. Karma and A. E. Lobkovsky, Phys. Rev. Lett. **92**, 245510 (2004).
[17]H. Henry and H. Levine, Phys. Rev. Lett. **93**, 105504 (2004).
[18]R. Spatschek, M. Hartmann, E. Brener, H. Mueller-Krumbhaar, and K. Kassner, Phys. Rev. Lett. **96**, 015502 (2006).
[19]Y. M. Jin, Y. U. Wang, and A. G. Khachaturyan, Appl. Phys. Lett. **79**, 3071 (2001).
[20]Y. U. Wang, Y. M. Jin, and A. G. Khachaturyan, J. Appl. Phys. **91**, 6435 (2002).
[21]Y. U. Wang, Y. M. Jin, A. M. Cuitino, and A. G. Khachaturyan, Acta Mater. **49**, 1847 (2001).
[22]X. P. Xu and A. Needleman, J. Mech. Phys. Solids **42**, 1397 (1994).
[23]K. Park, G. H. Paulino, and J. R. Roesler, J. Mech. Phys. Solids **57**, 891 (2009).
[24]V. I. Levitas, A. V. Idesman, and D. L. Preston, Phys. Rev. Lett. **93**, 105701 (2004).
[25]A. V. Idesman, V. I. Levitas, D. L. Preston, and J. Y. Cho, J. Mech. Phys. Solids **53**, 495 (2005).
[26]H. M. Zbib and E. C. Aifantis, Acta Mech. **92**, 209 (1992).
[27]P. Perzyna and K. Korbel, Acta Mech. **129**, 31 (1998).
[28]L. D. Landau and E. M. Lifshitz, *Statistical Physics* (Butterworth Heinemann, Oxford, 1980).
[29]L. D. Landau, *Collected Papers of L. D. Landau*, edited by D. Haar (Gordon and Breach, New York, 1965).
[30]V. I. Levitas, V. A. Levin, K. M. Zingerman, and E.I. Freiman, Phys. Rev. Lett. **103**, 025702 (2009).
[31]V. I. Levitas and D. L. Preston, Phys. Lett. A **343**, 32 (2005).
[32]V. I. Levitas and M. Javanbakht, Phys. Rev. Lett. **105**, 165701 (2010).
[33]V. I. Levitas and K. Samani, Nat. Commun. **2**, 284 (2011).
[34]V. I. Levitas and D. L. Preston, Phys. Rev. B **66**, 134206 (2002).
[35]V. I. Levitas and D. L. Preston, Phys. Rev. B **66**, 134207 (2002).